Available online at www.sciencedirect.com
SCIENCE DIRECT®
Optical Materials 26 (2004) 275–280
OPTICAL Materials
www.elsevier.com/locate/optmat

Microbial inhibition, growth of Li^+-doped LAP single crystals and their characterization

N. Kavitha [a], M. Arivanandhan [a], K. Ramamoorthy [a], K. Ragavendran [b], K. Sankaranarayanan [a,*]

[a] *Crystal Research Centre, Alagappa University, Karaikudi 630003, India*
[b] *Central Electrochemical Research Institute, Karaikudi 630003, India*

Received 23 September 2003; received in revised form 23 December 2003; accepted 10 January 2004
Available online 5 March 2004

Abstract

The addition of citric acid in the growth solution of LAP found to inhibits the microbial contamination and coloration of the solution with time exist in the growth of LAP by the conventional slow solvent evaporation technique. The stability study of the pure and citric acid mixed LAP solution at different temperature shows that the addition of citric acid has the advantage of extending the durability of the growth solution without coloration and convenience of usage for the growth of high-quality LAP crystals. Pure and Li^+-doped LAP crystals were grown by slow solvent evaporation technique and are characterized by X-ray powder diffraction, FTIR, thermal analysis (TGA, DTA) and AC impedance analysis. The presence of Li^+ in Li^+-doped LAP was measured by atomic absorption spectroscopy (AAS). The results suggested that tri-lithium citrate has the characteristics of lithium doping in LAP crystals and inhibits the microbial growth and coloration.

PACS: 42.70.Hj
Keywords: Nonlinear optical materials; LAP crystals; Solution growth

1. Introduction

L-arginine phosphate (LAP) [1], an amino-acid-based organic crystal is an important nonlinear optical compound due to its advantages such as three time larger nonlinearity, two or three times high laser damage threshold of KDP, chemical stability and also lower cost. But during the growth of LAP, the microbial contamination and coloration of the solution with time are the main disadvantages exist in the conventional slow solvent evaporation technique which restrict the growth of large size crystals. Since, L-arginine is an amino acid, which is rich in nutrient, microbes were found on the surface of the solution when exposed to atmosphere thereby inhibiting the growth of the crystals. A number of additives such as H_2O_2, $CHCl_3$, *n*-hexane, KF and liquid parafine have been tried to inhibit the microbial growth without harming the properties of the LAP [2–4].

A literature survey made in the field of lithium-based research works revealed that many of the physical properties of a particular material were enhanced by the addition of Li^+ ions. Lithium and lithium-based materials finds applications in the field of solid state rechargeable batteries at higher discharge rate [5], optical and acoustic devices, photorefractive materials and microwave applications [6]. Also, the influence of Li^+ ions in the glass matrix formation was studied and reported [7] to have sharp cutoffs in both UV–vis and IR regimes and these glasses may be useful in spectral devices. The observed high dielectric values compared to conventional glass forming were attributed to the lithium addition. Further, high polarizing power of Li^+ ion is responsible for many of the reported results. In this view, Li^+ ion was selected to introduce into the LAP matrix with the expectation to explore the lithium-ion

* Corresponding author. Tel.: +91-44-225205; fax: +91-44-225202.
E-mail address: hhrsankar@yahoo.com (K. Sankaranarayanan).

0925-3467/$ - see front matter © 2004 Elsevier B.V. All rights reserved.
doi:10.1016/j.optmat.2004.01.005

mobility. The tri-lithium citrate was selected as the source material for lithium dopant because they have extreme value of electronegativity ions Li^+ and can be made as aqueous solution.

In the present work, the effect of citric acid on the microbial inhibition and coloration of the solution was studied. The effect of lithium doping in LAP was analyzed by X-ray powder diffraction, FTIR and thermal analysis (TGA, DTA). The atomic absorption spectroscopy was used to measure the concentration of lithium in the grown Li^+-doped LAP single crystal. AC impedance analysis was conducted on the lithium-doped LAP single crystal to investigate the lithium-ion mobility.

2. Experimental procedure

Pure L-arginine phosphate was grown from aqueous solution using distilled water by slow solvent evaporation technique. An equimolar amount of L-arginine and orthophosphoric acid (AR grade) were mixed with excess water to synthesize L-arginine phosphate monohydrate and the obtained material was recrystallized twice in distilled water in order to improve its purity. Pure and 1 wt.% of citric acid mixed saturated solution of LAP were prepared by dissolving 35 g of LAP in 100 ml of distilled water and allowed for solvent evaporation. To find out the effect of microbial contamination and coloration of the solution with time that normally occurs in LAP family solutions, the prepared pure and citric acid mixed LAP solutions were monitored under the same growth environment. To grow lithium-doped LAP crystal, the glass vessels containing the saturated solutions of LAP was doped with 300 and 600 ppm of tri-lithium citrate. The addition of dopant and citric acid altered the saturation point of the solutions so that the once again saturation was realized. The LAP crystals obtained from citric acid mixed LAP and lithium-doped LAP were transparent, colorless and free from microbes, whereas microbial contamination observed in the pure solutions of LAP within two weeks resulted less transparent crystals. The crushed powder obtained from the transparent crystals of citric acid mixed LAP and lithium-doped LAP were subjected to X-ray powder diffraction, differential thermal analysis and thermo-gravimetric analysis and Fourier transform infrared spectroscopic analyses. The concentration of lithium in the grown crystal was calculated by atomic absorption spectroscopy. AC impedance analysis was conducted on the lithium-doped LAP single crystal (along (1 0 0) plane) placed in-between ion blocking and ion non-blocking electrodes such as stainless steel and lithium foils at different frequencies respectively. The AC impedance analysis was made by employing impedance analyzer, EG & G Princeton Applied Research, USA.

3. Results and discussion

The synthesized salts were dissolved in doubly distilled water. The solutions were saturated at 32 °C. The saturation was confirmed by using test seeds in the respective beakers. Saturated solutions of pure and doped LAP were filtered with fine filters and the growth was initiated at 32 °C by slow solvent evaporation technique. The grown pure and lithium-doped LAP crystals are shown in Fig. 1. In agreement with the observations made by earlier researchers, the morphology of the grown crystals consists of the forms {1 0 0}, {1 0 1}, {1 1 0}, {0 1 1} etc., while (1 0 0) habit face has a perfect cleavage [8,9] and the (1 0 0) plane of all the grown crystals are found to have more area than the other planes. The crystallographic directions can be readily identified from the crystal habit.

For growth rate analysis, the grown crystals were harvested at a specific period of time and the morphology of the grown crystals along the specific direction was compared. Growth rate analysis along the various planes of pure and doped LAP crystals is summarized as follows. The growth rate along the *c*-axis was found to be higher than the other two axes in pure and lithium-doped LAP crystals. In the case of tri-lithium citrate-doped LAP crystal, introduction of Li^+ in the LAP lattice, enhances the growth rate along the *c*-axis i.e., the growth rate along (0 0 1) direction of Li^+-doped LAP was faster than the pure LAP crystal. Also, the addition of Li^+ dopant increases the number of nucleations when compared to pure LAP crystal growth.

3.1. X-ray diffraction studies

The recorded X-ray powder diffraction spectrums using monochromatic intense X-ray of wavelength 1.5418 Å (CuK_α) for pure and lithium-doped LAP were presented in Fig. 2. The calculated lattice parameter data are presented in Table 1. The obtained intense and

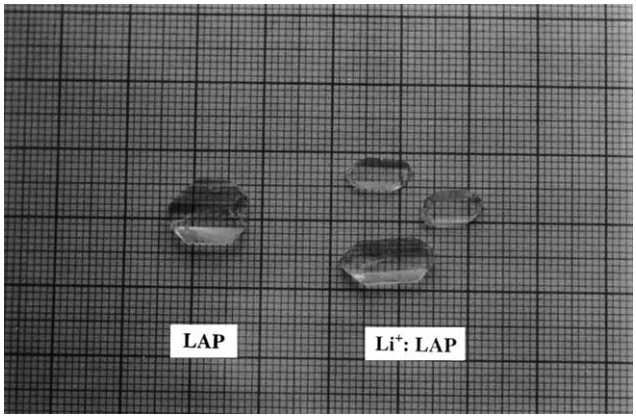

Fig. 1. Photograph of the grown pure and Li^+-doped LAP single crystals.

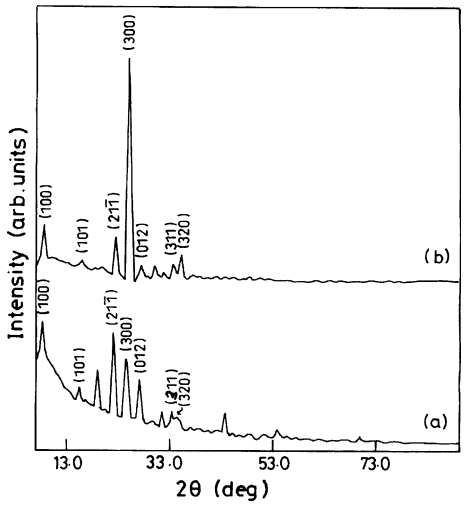

Fig. 2. X-ray diffraction spectrum of pure and Li^+-doped LAP single crystals. (a) For pure LAP, (b) for Li^+-doped LAP.

Table 1
Lattice parameter data for LAP and Li^+–LAP crystals

Sl. No.	Lattice parameter (Å)	Reported value (Å)	LAP (Å)	Li^+–LAP (Å)
1	*a*	10.75	10.78	10.82
2	*b*	7.91	7.50	7.54
3	*c*	7.32	7.38	7.47

sharp peaks in the diffractogram imply the crystalline quality of the grown pure and doped LAP crystals. The observed '*d*' values match with the reported value and confirm the material quality. In the case of lithium doped (2 ppm) LAP crystal, no marked change in 2θ values but the intensity of the (3 0 0) plane increases considerably. This indicates that the incorporation of lithium in the LAP lattice induces more growth rate along the (3 0 0) plane when compared to all other planes in the doped LAP crystal and more growth rate along (3 0 0) plane when compared to (3 0 0) plane of pure LAP crystal.

3.2. Microbial contamination and coloration

The addition of tri-lithium citrate in the growth solution of LAP found to inhibits the microbial contamination and coloration of the solution with time exist in the growth of LAP by the conventional slow solvent evaporation technique. Even though the growth experiments were conducted beyond 40 days yet the growth solution was free of microbial contamination and colorless. Hence, a stability study of the pure and citric acid mixed LAP solution at different temperature (room temperature, 35 and 40 °C) was carried out and found that the addition of citric acid has the advantage of extending the durability of the growth solution without coloration and convenience of usage for the growth of high-quality LAP crystals. In the present work, care has been taken to avoid the direct exposure of intense illuminations to the crystallizers in order to avoid photo-induced decomposition as reported by Dhanraj et al. [2] and Sasaki and co-workers [3]. Even then, a slight change in color was observed in the case of pure LAP after the growth period of 20 days.

3.3. Fourier transform infrared spectroscopy analysis

Figs. 3 and 4 represent the FTIR spectrums recorded on the grown crystals of pure and lithium-doped LAP (3.8 ppm in the crystal) in the range of 4000 and 400 cm^{-1} using KBr pellet by a Bruker IFS model 66 V spectrometer.

The FTIR spectrum recorded on the grown pure LAP single crystal was compared with the literature and found that the finger print region and the high-frequency absorption bands are in match with the reported spectrum, which confirms that the synthesized material contains all the reported functional groups. From the

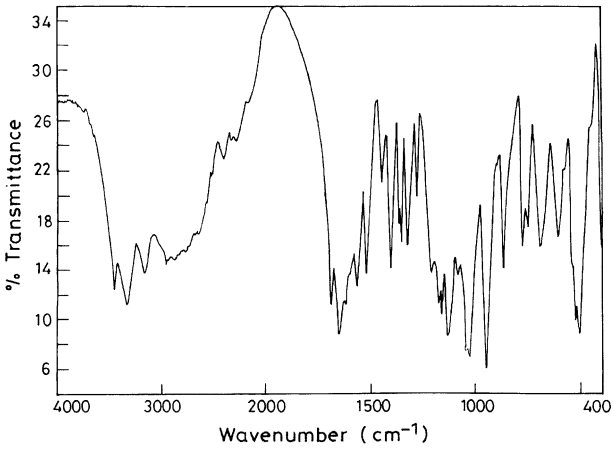

Fig. 3. FTIR spectrum for grown pure LAP sample.

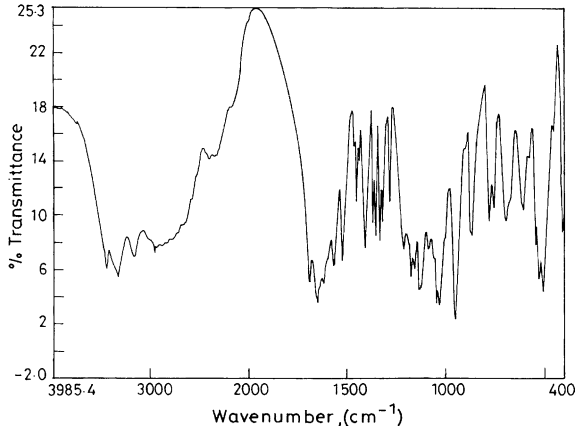

Fig. 4. FTIR spectrum for grown Li^+-doped LAP crystal.

recorded spectrum, the following functional groups were assigned. The high-frequency range of the spectrum consists of bands which are due to the NH_2, NH_2^+, NH_3^+, COO^- and HPO_4^- stretching vibrations. The bonds observed in the lower frequency regions were due to the deformation vibrations of various functional groups.

In FTIR spectrum, the bands are formed due to the internal vibration of the arginine molecule, phosphate group and hydrated water group. Moreover, rocking mode, symmetric deformation and asymmetric bending were found from the spectrum. The scissoring mode of COO^- group is at 770 cm^{-1}. In the formation of phosphate ion, P–OH stretching was formed at 950 and 1032 cm^{-1}. P–OH deformation bands are due to the internal vibration of the phosphate group, which are observed around 408 and 506 cm^{-1}, respectively. Table 2 summarizes the various functional group assignments made on the recorded FTIR spectrum of pure LAP. The missing peaks of v_3 (PO_4) and v_4 (PO_4) vibrations corresponding to 1100 and 525 cm^{-1} respectively (compared to the reported data) may be due to the weak interaction of phosphate group with the carboxylic group in LAP.

Earlier IR absorption studies on lithium based materials, observed a high-frequency band in the range of 600–580 cm^{-1} and a second absorption band in the range of 400–385 cm^{-1} [10]. When compared to the recorded FTIR spectrum of pure LAP, no major difference was observed in the FTIR spectrum of lithium-doped LAP crystal. Hence, the following remarks can be derived when the FTIR spectrums of pure LAP, Li^+-doped LAP and tri-lithium citrate were compared. The absence of noticeable changes in the high-frequency region and in the finger print region of lithium-doped LAP indicates that the lithium-doped LAP retains the structure of pure LAP with lithium ions in the interstitial sites.

3.4. Atomic absorption spectroscopy (AAS) studies

In order to calculate the doping concentration of lithium ions in the lithium-doped LAP, the atomic absorption spectroscopy study was made. The calculated lithium ion concentrations in the grown crystals were 2.1 and 3.8 ppm corresponding to 370 and 600 ppm of lithium ion concentration in the growth solution, respectively. Increasing the lithium ion concentration in the growth solution enhances the lithium ion concentration in the grown crystal. In general, concentration of the dopant in the grown crystal mainly depends on the available dopant concentration in the vicinity of the growing layer that largely depends on the experimental conditions exists during the growth.

3.5. Thermal studies

Fig. 5 illustrates the DTA and TGA thermal analyses curves for lithium doped LAP (2.1 ppm) crystal. From the DTA curve, an irreversible endothermic transition at 116 °C was observed where the decomposition begins. The peak of the endothermic transition represents the melting point of the material i.e., at 134 °C. Between 116 and 134 °C, lithium-doped LAP crystal starts to soften and then fully melts. The TG curve at 151 °C shows a loss of weight of 4%, which mainly attributed to the loss of water. In the case of lithium-doped LAP, the decomposition temperature is decreased by 3 °C when compared to the reported decomposition temperature (137 °C) of pure LAP [11]. The reduction in decompo-

Table 2
Wave number assignment for the pure and Li^+–LAP crystals

Sl. No.	Literature value (cm^{-1})	Observed value (cm^{-1})	Functional group assignment
1	3450	3450.09	$v_3(H_2O)$
2	3330	3333.84	$v_1(H_2O)$
3	3160	3166.60	NH_3^+ asymmetric stretching
4	1690	1690.32	C=N stretching
5	1650	1651.80	NH_2^+ deformation
6	1570	1569.24	COO^- asymmetric stretching
7	1530	1524.93	NH_3^+ asymmetric stretching
8	1450	1453.48	$v_2(H_2O)$
9	1410	1408.65	COO^- asymmetric stretching
10	1370	1370.27	C–C–H in plane deformation
11	1330	1333.43	CH_2 wagging
12	1290	1285.77	P–OH angular
13	1180	1175.67	NH_3^+ rocking
14	1160	1159.87	NH_2 wagging
15	1035	1031.67	P–OH deformation
16	960	950.38	P–OH stretching
17	885	873.65	C–C stretching, P–OH stretching
18	790	781.32	NH_2^+ rocking
19	770	761.03	COO^- scissoring
20	623	614.6	OH out of plane deformation

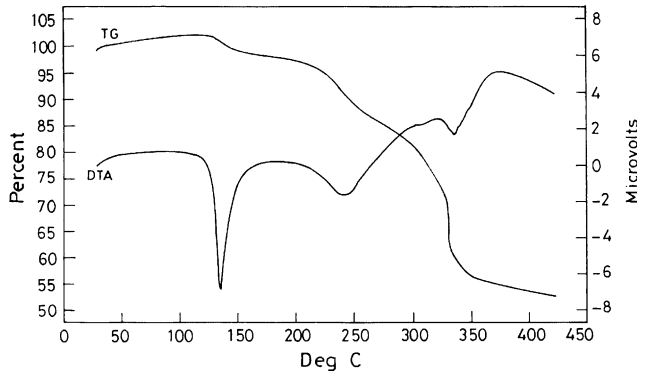

Fig. 5. TG and DTA curves for Li^+-doped LAP crystal.

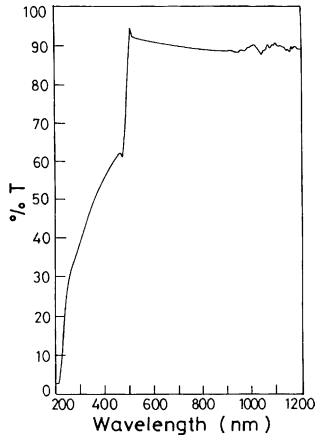

Fig. 6. UV–vis transmission spectra of Li^+-doped LAP single crystals.

sition temperature is due to the decreased bond energy caused by the addition of Li^+ ions.

3.6. Optical transmission studies

The optical transmittance study made on the grown lithium-doped LAP (2.1 ppm) single crystal was presented in Fig. 6. From the figure, the near zero transmittance below the cutoff wavelength at 210 nm, and the high degree of transparency (90%) in the wavelength of 450–1200 nm illustrates the optical quality of the grown lithium-doped LAP crystal.

3.7. AC impedance analysis

AC impedance analysis was conducted on the lithium-doped LAP (3.8 ppm) specimen (cut parallel to (1 0 0) plane) placed in between ion blocking (stainless steel) and ion non-blocking (lithium) electrodes in the frequency range of 100 kHz to 10 MHz and the corresponding impedance values were measured and presented in Fig. 7a and b. The calculated resistance and capacitance values of the sample using ion blocking (stainless steel) and ion non-blocking (lithium) electrodes are as follows: $R = 3.91 \times 10^9\ \Omega/C = 2.51 \times 10^{-11}$ F and $R = 2.7 \times 10^9\ \Omega/C = 4 \times 10^{-11}$ F, respectively. The observed small difference in the conductivity of lithium-doped LAP between these experiments suggested a low lithium ion mobility in the crystal.

In conclusion, good optical quality crystals of pure and lithium-doped LAP crystal were grown. An additive of Li^+ ion enhances the growth rate along the *c*-axis as confirmed by the X-ray powder diffraction studies. Also, the small variations in the lattice parameter values are due to the contribution of Li^+ ion additives in the interstitial sites. The FTIR analysis confirms the presence of various characteristic functional groups such as NH_2, NH_2^+, NH_3^+, COO^- and H_2PO_4 in LAP and lithium-doped LAP. DTA and TG curves explained the thermal behavior of lithium-doped LAP crystal and shows decomposition temperature decreased by 3 °C when compared to pure LAP. This may be attributed to the changes in the bond strength of the LAP molecule by the inclusion of lithium ions.

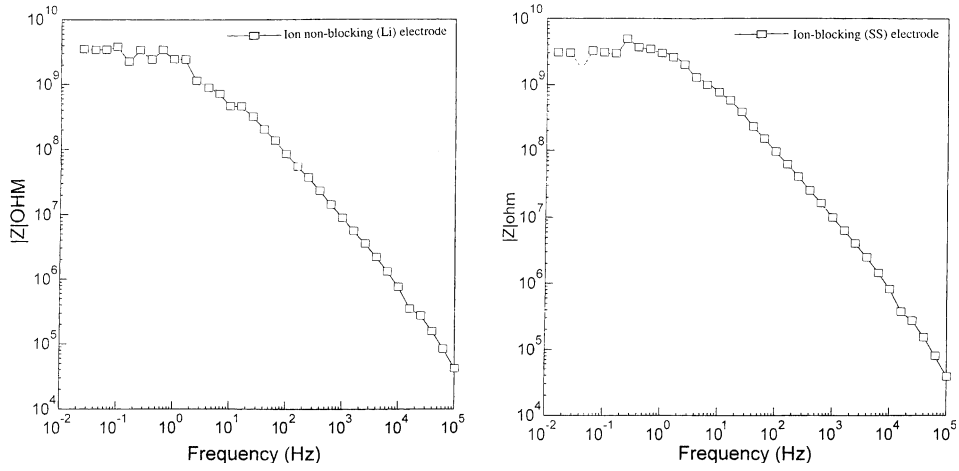

Fig. 7. (a) Impedance curve for Li^+-doped LAP single crystal using ion blocking electrodes. (b) Impedance curve for Li^+-doped LAP single crystal using ion non-blocking electrodes.

The presence of lithium ion in the grown lithium-doped LAP crystal was confirmed and measured by the atomic absorption spectroscopy. From optical transmittance studies, the attained high degree of transmittance value in the range of 450–1200 nm illustrates the optical quality of the grown crystal. AC impedance analysis using ion blocking and ion non-blocking electrodes indicated low lithium ion mobility in the grown crystal. Finally, the obtained results suggested that trilithium citrate has the characteristics of lithium doping in LAP crystals and inhibits the microbial growth and coloration.

Acknowledgements

Authors are grateful to Dr. A. Muthukumaran and Mr. K. Kulangiyappar, Central Electrochemical Research Institute, Karaikudi for their timely help.

References

[1] D. Xu, M. Jingo, Z. Tan, Acta Chem. Sin. 41 (1983) 570.
[2] G. Dhanaraj, T. Shripathi, H.L. Bhat, J. Crystal Growth 113 (1991) 456.
[3] A. Yokotani, T. Sasaki, K. Fujioka, S. Nakai, C. Yamanaka, J. Crystal Growth 99 (1990) 815.
[4] A.S. Haja Hameed, G. Ravi, P. Ramasamy, J. Crystal Growth 229 (2001) 547.
[5] J.S. Sakamoto, B. Dunn, J. Mater. Chem. 122 (2002) 859.
[6] A.M. Shaikh, S.C. Watawe, S.A. Jablhar, B.K. Ckougule, Mater. Res. Bull. 37 (2002) 2547.
[7] S. Hazra, S. Mandal, A. Ghosh, J. Phys. Rev. B 56 (13) (1997) 8021.
[8] G. Ravi, K. Srinivasan, S. Anbukumar, P. Ramasamy, J. Crystal Growth 137 (1994) 598.
[9] W.J. Liu, C. Ferrari, M. Zha, L. Zanotti, S.S. Jiang, Cryst. Res. Technol. 35 (2000) 1215.
[10] A.M. Shaikh, S.A. Jadhav, S.C. Watawe, B.K. Chougule, Mater. Lett. 44 (2000) 192.
[11] A.S. Haja Hameed, G. Ravi, M.D.M. Hossain, P. Ramasamy, J. Crystal Growth 204 (1999) 333.